Title

Ethanol Consumption Induces Nonspecific Inflammation and Functional Defects in Alveolar Macrophages.

Journal

American Journal of Respiratory Cell and Molecular Biology, 67(1)

ISSN

1044-1549

Authors

Lewis, Sloan A

Doratt, Brianna M

Sureshchandra, Suhas

et al.

Publication Date

2022-07-01

DOI

10.1165/rcmb.2021-0346oc

ORIGINAL RESEARCH

Ethanol Consumption Induces Nonspecific Inflammation and Functional Defects in Alveolar Macrophages

Sloan A. Lewis[1,2], Brianna M. Doratt[1,3], Suhas Sureshchandra[1,2], Allen Jankeel[1], Natali Newman[4], Weining Shen[5], Kathleen A. Grant[4], and Ilhem Messaoudi[1,2,3]

[1]Department of Molecular Biology and Biochemistry, [2]Institute for Immunology, and [5]Department of Statistics, University of California, Irvine, Irvine, California; [3]Department of Microbiology, Immunology, and Molecular Genetics, College of Medicine, University of Kentucky, Lexington, Kentucky; and [4]Oregon National Primate Research Center, Oregon Health and Science University, Beaverton, Oregon

ORCID ID: 0000-0003-3203-2405 (I.M.).

Abstract

Chronic alcohol drinking is associated with increased susceptibility to viral and bacterial respiratory pathogens. In this study, we use a rhesus macaque model of voluntary ethanol self-administration to study the effects of long-term alcohol drinking on the immunological landscape of the lung. We report a heightened inflammatory state in alveolar macrophages (AMs) obtained from ethanol (EtOH)-drinking animals that is accompanied by increased chromatin accessibility in intergenic regions that regulate inflammatory genes and contain binding motifs for transcription factors AP-1, IRF8, and NFKB p-65. In line with these transcriptional and epigenetic changes at the basal state, AMs from EtOH-drinking animals generate elevated inflammatory mediator responses to lipopolysaccharides and respiratory syncytial virus. However, the transcriptional analysis revealed an inefficient induction of interferon-stimulated genes with EtOH in response to the respiratory syncytial virus, suggesting disruption of antimicrobial defenses. Correspondingly, AMs from EtOH-drinking animals exhibited transcriptional shifts indicative of increased oxidative stress and oxidative phosphorylation, which was coupled with higher cytosolic reactive oxygen species and mitochondrial potential. This heightened oxidative stress state was accompanied by decreased ability to phagocytose bacteria. Bulk RNA and assay for transposase-accessible chromatin sequencing data further revealed reduced expression and chromatin accessibility of loci associated with tissue repair and maintenance with chronic EtOH drinking. Similarly, analysis of single-cell RNA sequencing data revealed shifts in cell states from tissue maintenance to inflammatory responses with EtOH. Collectively, these data provide novel insight into mechanisms by which chronic EtOH drinking increases susceptibility to infection in patients with alcohol use disorders.

Keywords: alcohol; lung; macrophages; scRNA-Seq; ATAC-Seq

Alcohol use is prevalent in the United States, with over 50% of people 18 years or older reporting alcohol consumption within the previous 30 days (National Survey on Drug Use and Health 2019). Among these individuals, 25% report binge drinking, and 6.3% report heavy drinking. Long-term heavy drinking is associated with numerous adverse health outcomes, including increased incidence of cardiac disease (1, 2), certain types of cancer (3–6), liver cirrhosis (7), and sepsis (8), making it the third leading preventable cause of death in the United States (9). Of importance, chronic heavy alcohol drinking compromises lung health and immunity, leading to increased susceptibility to both bacterial and viral pulmonary infections (10), notably

(Received in original form August 2, 2021; accepted in final form April 5, 2022)

Supported by grants from The National Institute on Alcohol Abuse and Alcoholism at the National Institutes of Health (1R01AA028735-01 [I.M.], 5U01AA013510-20, and 2R24AA019431-11); S.A.L. is supported by grant 1F31A028704-01. The content is solely the responsibility of the authors and does not necessarily represent the official views of the National Institutes of Health.

Author Contributions: S.A.L., K.A.G., and I.M. conceived and designed the experiments. S.A.L., B.M.D., A.J., S.S., and N.N. performed the experiments. S.A.L. and B.M.D. analyzed the data. W.S. assisted with statistical analysis. S.A.L. and I.M. wrote the paper. All authors have read and approved the final draft of the manuscript.

The datasets supporting the conclusions of this article are available on National Center for Biotechnology Information's (NCBI's) Sequence Read Archive (PRJNA767842).

Correspondence and requests for reprints should be addressed to Ilhem Messaoudi, Ph.D., Department of Microbiology, Immunology, and Molecular Genetics, College of Medicine, University of Kentucky, Lexington, KY 40536-0679. E-mail: ilhem.messaoudi@uky.edu.

This article has a data supplement, which is accessible from this issue's table of contents at www.atsjournals.org.

Am J Respir Cell Mol Biol Vol 67, Iss 1, pp 112–124, July 2022

Originally Published in Press as DOI: 10.1165/rcmb.2021-0346OC on April 5, 2022
Internet address: www.atsjournals.org

respiratory syncytial virus (RSV) (11), community-acquired pneumonia (12–14), and tuberculosis (15, 16). Alcohol use is also a risk factor for acute respiratory distress syndrome (17, 18) and admission to the ICU in patients with pneumonia (10, 12, 17, 19). Although the mechanisms underlying increased vulnerability and severity of pulmonary infections with chronic alcohol consumption have yet to be fully elucidated, studies using rodent models as well as *in vitro* cell cultures have identified defects in the beating of the ciliated epithelium (20–22) as well as impaired epithelial barrier function (23, 24) as major risk factors. Moreover, these studies report significant defects in both the innate and adaptive branches of the immune system (10), especially within alveolar macrophages (AMs), the first line of defense in the lung (25). Specifically, prolonged alcohol exposure alters the ability of AMs to release cytokines and chemokines needed to recruit immune cells into the lung (26, 27) as well as their ability to clear both microbes and dying cells to reduce damage to tissue (28), potentially owing to oxidative stress (29). However, the molecular bases for altered lung macrophage function by chronic alcohol consumption remain poorly defined.

Lung-resident macrophages can be categorized into interstitial macrophages primarily residing within the tissue and AMs predominantly found within the lumen of the alveoli (30–35). Studies in mice have revealed that lung macrophages are derived from the yolk sac and fetal liver as well as from bone marrow monocytes (36, 37). It is believed that embryonically derived macrophage populations have a self-renewal capacity and are functionally distinct from the monocyte-derived macrophage populations; however, whether this is true in humans is still unanswered (30). Recent studies have uncovered enormous heterogeneity in lung macrophage populations, but the mechanisms by which environmental factors or inflammatory settings alter the ability of these cells to clear pathogens and repair tissue remain poorly understood.

In this study, we use BAL samples collected from rhesus macaques that voluntarily self-administered ethanol (EtOH) or an isocaloric solution for 12 months to examine the alcohol-induced epigenetic and transcriptomic underpinnings of altered macrophage function. Although AMs from EtOH-drinking animals generate a heightened inflammatory response to lipopolysaccharides (LPSs) and RSV, they exhibit a dampened antiviral transcriptional response to RSV and reduced phagocytosis of bacterial particles compared with AMs from control animals. Additional transcriptional analyses revealed shifts toward heightened inflammation and oxidative stress and away from tissue repair. These transcriptional and functional changes were accompanied by epigenetic alterations at baseline, in which genomic regions associated with immune cell activation and degranulation were more accessible, whereas those associated with tissue maintenance/repair and cell migration were less accessible.

Some of the results of these studies have been previously reported in the form of a preprint (bioRxiv, [31 July 2021] https://doi.org/10.1101/2021.07.30.454528).

Methods

See the data supplement for detailed methods.

Animal Studies and Sample Collection

These studies used blood and BAL samples from 11 female and 8 male rhesus macaques (average age 5.68 yr; 9 control animals and 10 chronic heavy drinkers). BAL cells were obtained after 12 months and cryopreserved until they could be analyzed as a batch. Cohort information is outlined in Table E1 in the data supplement.

Flow Cytometry Analysis

BAL cells were stained with the indicated surface antibodies, acquired with an Attune NxT Flow Cytometer, and analyzed using FlowJo software.

Monocyte/Macrophage Stimulation Assays

Cells from the BAL (6.5×10^4 FACS sorted $CD206^+$) were cultured with or without 100 ng/ml LPS or RSV at a multiplicity of infection of 5 for 16 hours. Supernatants from stimulated AMs were measured using a 31-plex panel of indicated factors.

Bulk RNA Sequencing (RNA-Seq) Library Preparation and Data Analysis

Libraries from peripheral blood mononuclear cell RNA were generated using the TruSeq Stranded RNA LT kit. Libraries from purified $CD14^+$ monocyte RNA were generated using the NEBnext Ultra II Directional RNA Library Prep Kit. Libraries were multiplexed and sequenced on the NovaSeq platform. RNA-Seq reads were quality checked and trimmed and aligned to the *Macaca mulatta* genome (8.0.1). Read counts were normalized using the RPKM (reads per kilobase of transcript, per million mapped reads) method. Differentially expressed genes (DEGs) were identified using edgeR (38) (Table E5). Functional enrichment of DEGs was performed using Metascape (39).

Assay for Transposase-Accessible Chromatin Sequencing (ATAC-Seq) Library Preparation and Data Analysis

AMs were subjected to nuclei isolation, transposition, and amplification for ATAC-Seq. Libraries were multiplexed and sequenced to a depth of 50 million 100 bp paired reads. Reads were quality checked, trimmed, and aligned to the *Macaca mulatta* genome (8.0.1). Mitochondrial reads and PCR duplicate artifacts were removed. Samples from each group were concatenated, and accessible chromatin peaks were called using Homer's *findPeaks* function (40) (false discovery rate [FDR] < 0.05), and differential peak analysis was performed using Homer's *getDifferentialPeaks* function ($P < 0.01$) (Table E5).

10X 3′ Single-Cell RNA Sequencing (scRNA-Seq) Library Preparation and Analysis

Cells were loaded onto a 10X Chromium Controller. cDNA amplification and library preparation (10X v3.1 chemistry) were performed according to manufacturer protocol and sequenced on a NovaSeq S4 to a depth greater than 30,000 reads/cell. Sequencing reads were aligned to the *Macaca mulatta* (8.0.1) reference genome using Cell Ranger v3.1 (10X Genomics). Quality control steps were performed before downstream analysis with Seurat v3.2.2 (41), in which cells with fewer than 200 unique features (ambient RNA) and cells with greater than 20% mitochondrial content (dying cells) were removed. The pseudotime trajectory of the AMs/monocytes was reconstructed using Slingshot (42). Differential expression analysis was performed using MAST (Model-based Analysis of Single-Cell Transcriptomics) under default settings in Seurat. Gene signatures and pathways from Kyoto Encyclopedia of Genes and Genomes (KEGG) (https://www.genome.jp/kegg/pathway.html) (Table E4) were compared using Seurat's *AddModuleScore* function.

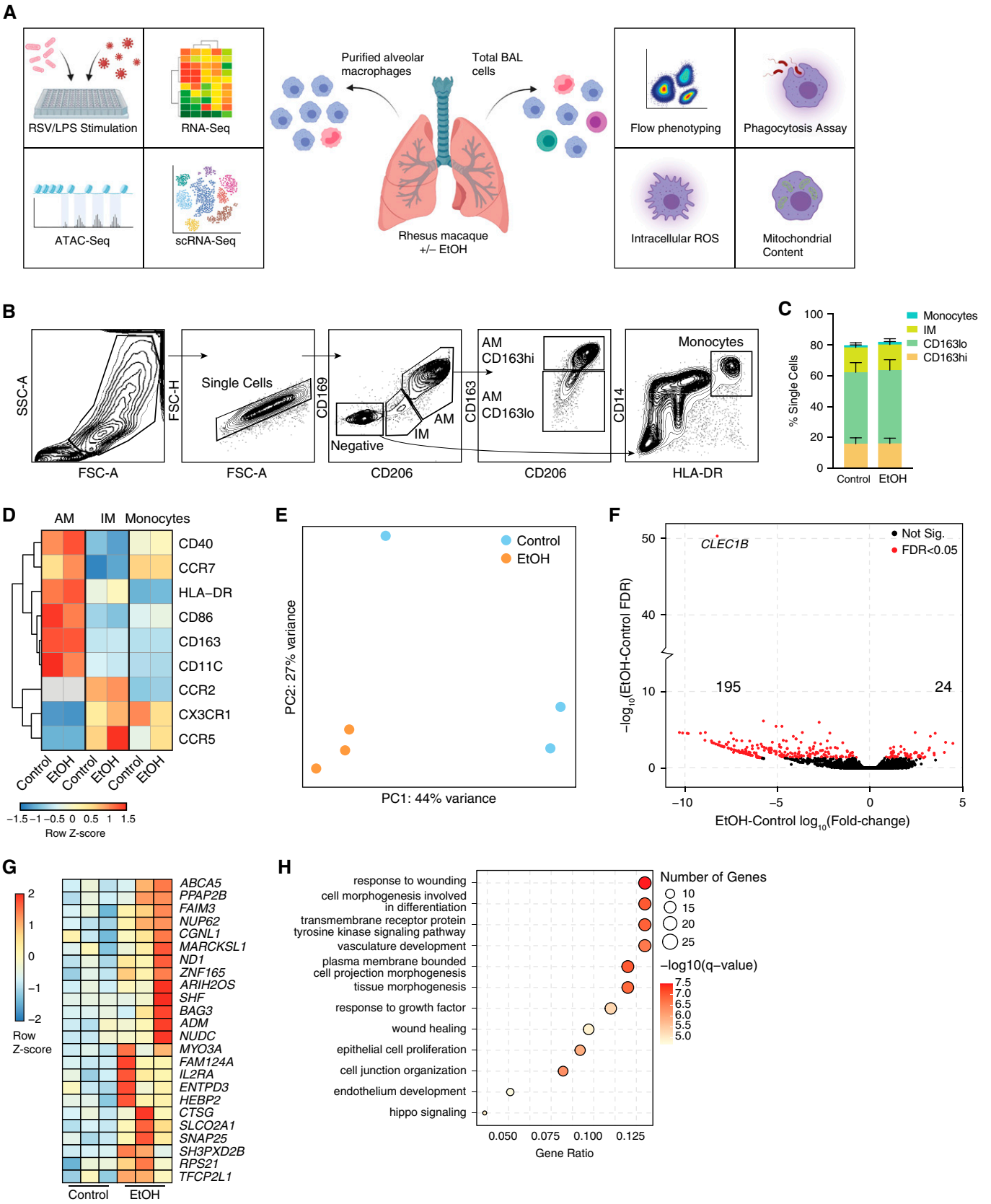

Figure 1. Chronic ethanol (EtOH) drinking induces changes in the alveolar macrophage (AM) transcriptome. (*A*) Experimental design of this study was created with BioRender.com. (*B*) Gating strategy to identify monocytes, IMs, and AMs from BAL samples. (*C*) Relative distributions

Macrophage Functional Assays

Mitochondrial membrane potential, intracellular reactive oxygen species (ROS), and phagocytosis were measured using MitoTracker Red CMXRos, CellRox Deep Red Reagent, and pHrodo Red *Staphylococcus aureus* BioParticles, respectively (Thermo Fisher/Invitrogen).

Statistical Analysis

All statistical analyses were conducted in GraphPad Prism 7.

Results

Chronic EtOH Drinking Skews AM Transcriptional Profiles Away from Tissue Repair

The alveolar space in the lung is home to a large population of tissue-resident macrophages and infiltrating monocytes that are the first responders to respiratory infections. Given that patients with alcohol use disorders have increased susceptibility to respiratory pathogens, we used a multipronged approach to uncover the pleiotropic impact of chronic heavy drinking on the transcriptional, epigenetic, and functional landscape of the AMs. We collected BAL samples from male and female rhesus macaques that consumed EtOH or an isocaloric solution daily for 12 months (Figure 1A; Table E1). The genetically diverse background of the outbred macaques and the voluntary ethanol self-administration make this a robust model of human drinking but could lead to significant intragroup variability (Table E1).

We first determined the impact of chronic EtOH on the phenotype of AMs by profiling cell surface markers using flow cytometry ($n = 6$ control animals, 8 EtOH animals). On the basis of previous studies (43–45), we identified AMs as $CD206^+$ $CD169^+$, interstitial macrophages as $CD206^+$ $CD169^-$, and infiltrating monocytes as $CD206^-CD169^-CD14^+$ $HLA\text{-}DR^+$ (Figure 1B). AMs were further subdivided on the basis of the expression of CD163 (Figure 1B). No significant differences in frequencies of these major macrophage/monocyte populations were observed after 12 months of chronic EtOH consumption (Figure 1C). Examination of surface activation markers and chemokine receptors revealed higher expression of CD40, CCR7, HLA-DR, CD86, CD163, and CD11C on AMs than interstitial macrophages or monocytes (Figure 1D). On the other hand, interstitial macrophages and monocytes expressed higher levels of CCR2, CX3CR1, and CCR5 compared with AMs (Figure 1D). Interestingly, chronic EtOH drinking led to a modest increase in the expression of the activation marker CD40 on the CD163lo AM subset (FDR $P = 0.07$) (Figure E1A). Therefore, chronic EtOH consumption over 12 months did not lead to statistically significant changes in frequency and phenotype of lung macrophages.

We have previously reported significant alterations in the transcriptional profiles of peripheral monocytes and splenic macrophages with chronic alcohol drinking (46–48). Therefore, we examined transcriptional changes within AM using bulk RNA sequencing of purified cells ($n = 3$/group) (Figures 1E–1H). Although considerable heterogeneity was noted in the control samples (Figure 1E), differential gene expression analysis revealed 24 genes to be upregulated with EtOH (Figure 1F), including *CTSG*, *SNAP25*, and *MYO3A*, which play a role in granulocyte activation and degranulation (49, 50) (Figure 1G). EtOH drinking was also associated with 195 downregulated DEGs, notably *CLEC1B*, which is associated with an antiinflammatory macrophage phenotype (Figure 1F) (51). Functional enrichment showed that the downregulated DEGs mapped significantly to gene ontology (GO) terms "response to wounding" (e.g., *CLEC1B*, *NRP1*, *PTK2*, and *PRKACB*), "cell morphogenesis" (e.g., *MYO7A* and *PLCGG1*), and "vasculature development" (e.g., *HMGA2* and *ACTA2*) pathways (Figure 1H; Figure E1B). These observations suggest that chronic EtOH drinking skews AMs away from tissue maintenance and repair and toward an inflammatory transcriptional state.

Chronic EtOH Drinking Alters the Epigenetic Landscapes of AMs

Previous studies have indicated that chronic EtOH consumption leads to epigenetic changes within monocytes and splenic macrophages (46, 48). To assess the impact of chronic EtOH consumption on the epigenome of AM, we performed ATAC-Seq on AMs purified from control and EtOH animals ($n = 3$/group). Although the relative distribution of open promoter and distal regions was comparable between groups (Figure 2A), several differentially accessible regions (DARs) were identified within the promoter and distal intergenic regions (Figure 2B). The 70 genes regulated by promoters that were closed with EtOH enriched to GO terms associated with barrier function such as "endothelium development" (e.g., *CLDN3* and *CLDN5*) and "regulation of cell junction assembly" (e.g., *DMNT*) as well as "T-helper cell differentiation" (e.g., *FOXP1*) (Figure 2C). The 25 genes associated with promoters that were more accessible with EtOH mapped to the GO term "regulation of hormone levels" (e.g., *CTSG*, *SNAP25*, and *MYO3A*) (Figures 2C and 2D). Intriguingly, the expression of these three genes was also upregulated on the basis of the bulk RNA-Seq analysis (Figure 2D).

Analysis of potential cis-regulatory mechanisms of regulation in the nonpromoter regions was performed by first lifting the genomic regions from the macaque genome to the human genome, followed by enrichment using the GREAT (Genomic Regions Enrichment of Annotations Tool) database. This analysis

Figure 1. (*Continued*). of the three myeloid cell subsets in the BAL. (*D*) Heatmap showing averaged median fluorescence intensity (MFI) values for cell surface markers in each indicated subset/group. The scale is row *Z*-score in which blue is the lower and red is the higher expression. (*E*) $CD206^+$ alveolar macrophages ($n = 3$/group) were purified from total BAL using FACS and subjected to bulk RNA sequencing (RNA-Seq). Principal component analysis of bulk RNA-Seq libraries from control and EtOH AMs. (*F*) Volcano plot representing the up and downregulated differentially expressed genes (DEGs) (false discovery rate [FDR] <0.05) in which the *x*-axis is $\log_{10}$ fold-change, and the *y*-axis is $-\log_{10}$ FDR. (*G*) Heatmap representing the expression of all DEGs upregulated with EtOH in which the scale is row *Z*-score representing low (blue) and high (red) expression. (*H*) Bubble plot showing gene ontology (GO) biological process enrichment of downregulated DEGs with EtOH compared with control animal. The size of the bubble represents the number of genes associated with that term, the color represents the $-\log_{10}$ *q*-value, and the *x*-axis is the ratio of genes mapping to that term to total genes. ATAC-Seq = assay for transposase-accessible chromatin sequencing; IM = interstitial macrophages; LPS = lipopolysaccharides; ROS = reactive oxygen species; RSV = respiratory syncytial virus; scRNA-Seq = single-cell RNA sequencing.

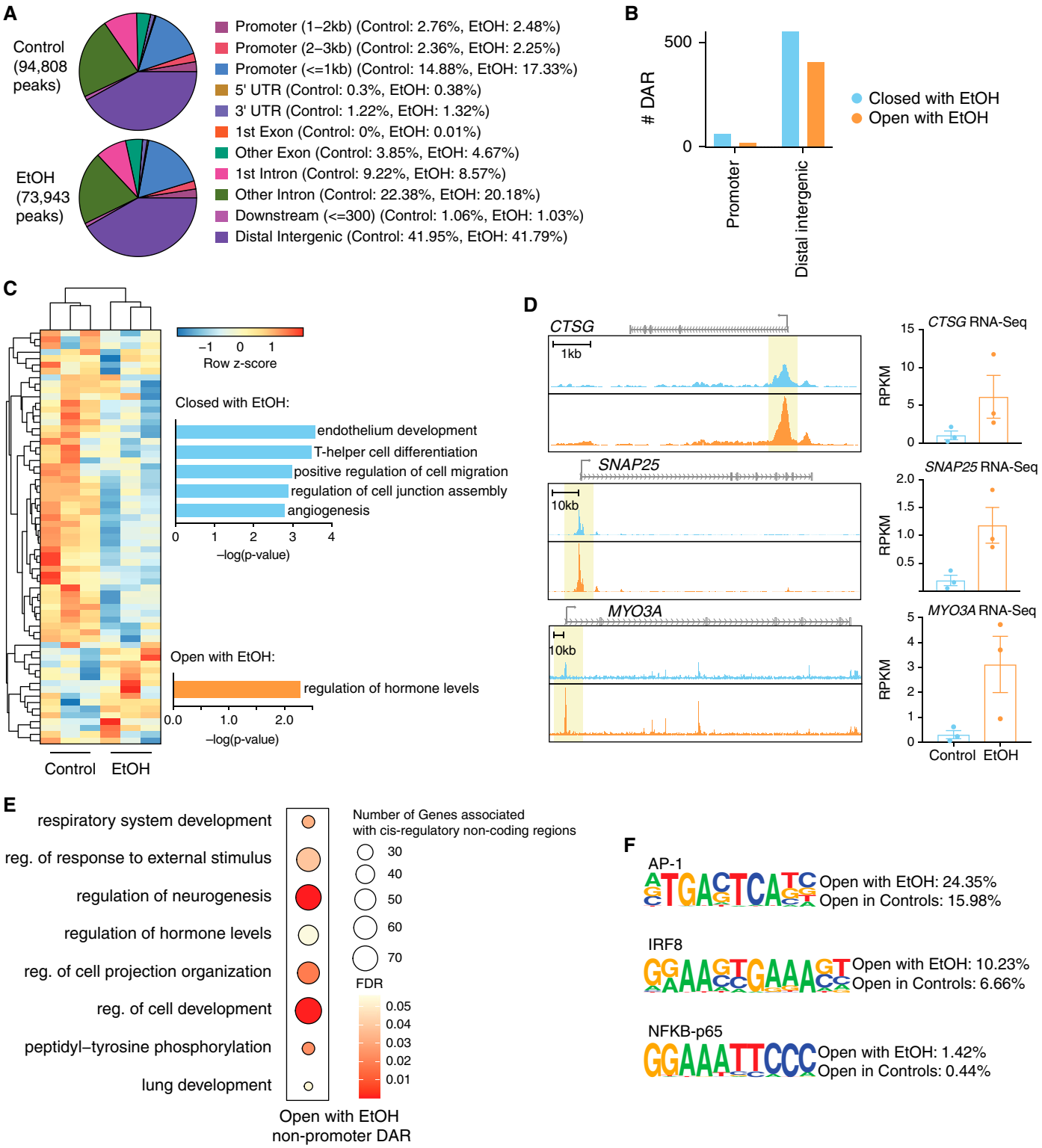

Figure 2. Epigenomic analysis of AMs with chronic EtOH drinking. AMs ($n = 3$/group) were purified from total BAL by $CD206^+$ sort, and nuclei were subjected to ATAC-Seq. (*A*) Pie charts showing genomic feature distribution of the open chromatin regions (fold-change ⩾ 2, FDR ⩾ 0.05) in control and EtOH AMs. (*B*) Bar chart showing the number of open and closed differentially accessible regions (DARs) (FDR ⩾ 0.01) with EtOH in promoter and distal intergenic regions. (*C*) Heatmap representing the open and closed (control EtOH) differentially accessible promoter region (FDR ⩾ 0.01) counts in which the scale is row *Z*-score representing low (blue) and high (red) expression. Bar plots to the right represent the functional enrichment of those promoter DARs in which the *x*-axis is $-\log_{10} P$ value. (*D*) Pile-ups of selected promoter DARs more open with

revealed no significant enrichment of the regions that were closed with chronic EtOH. On the other hand, intergenic regions that were more open with chronic EtOH drinking significantly enriched to "respiratory system development" (e.g., *CTGF*, *EGFR*, and *TGFBR2*) and "regulation of response to external stimulus" (e.g., *C1QB*, *CD180*, *CXCR4*, and *IL21*) (Figure 2E). Finally, we performed transcription factor (TF) binding motif analysis on the distal intergenic DAR, which showed a higher likelihood of binding sites for TF that play a critical role in inflammation, notably AP-1, IRF8, and NFKB p-65 in regions that are more accessible with chronic EtOH (Figure 2F). These observations indicate that chronic EtOH drinking leads to alteration in chromatin accessibility that results in AMs poised toward inflammatory responses and away from tissue repair and adaptive immune activation.

AMs Generate a Heightened Inflammatory Response but Compromised Interferon-induced Transcriptional Response with Chronic EtOH

Previous studies have reported an exaggerated inflammatory response by myeloid cells to LPS with chronic alcohol drinking (46, 48, 52, 53). Thus, we stimulated FACS-purified AMs with LPS ($n = 6$/group) and determined immune mediator production by Luminex (Figure E2A; Table E2). As previously described for peripheral blood monocytes and splenic macrophages (46, 48), AMs from EtOH-drinking animals mounted a hyperinflammatory response as indicated by heightened production of cytokines (IL-6, TNFα) and chemokines (CXCL8, CXCL10, CCL2, CCL4) compared with control AMs (Figure E2A). We next examined the responses of AMs to a respiratory pathogen. Purified AMs were stimulated with RSV *ex vivo* ($n = 8$/group), and antiviral responses were determined using Luminex and RNA-Seq. In response to RSV stimulation, AMs from control animals secreted several growth factors (BDNF [brain-derived neurotrophic factor], VEGF [vascular endothelial growth factor], PDGF [platelet-derived growth factor], and FGF [fibroblast growth factor]), a few chemokines (CCL5 and CXCL10), and canonical inflammatory marker IL-6 (Figure 3A). Despite comparable viral loads (Figure E2B), AMs from EtOH-consuming animals (but not control animals) produced significantly higher amounts of cytokines (IL-1β, IL-12, IL-15, IFNβ, IL-7) and growth factors (GM-CSF [granulocyte-macrophage colony-stimulating factor] and G-CSF [granulocyte colony-stimulating factor]) relative to their unstimulated condition (Figure 3A). AMs from EtOH-consuming animals also produced significantly higher concentrations of IL-6, IL-12, and TGFα relative to their control animal counterparts (Figure 3B). Moreover, significant positive correlations between IL-6, IL-12, and CCL5 concentration and EtOH dose were observed (Figure 3C).

In contrast to the immune mediator production profile, fewer upregulated DEGs were detected in AMs from the EtOH group compared with control animals (516 DEGs in control animals vs. 340 DEGs in the EtOH animals) (Figure 3D). DEGs upregulated only in the control animal group enriched to GO terms "regulation of innate immune response," "regulation of response to cytokines," and "response to IFNβ and IFNγ" (Figure 3E), whereas those upregulated in the EtOH group enriched to GO terms "cell cycle processes" and "cellular response to drug" (Figure 3E; Figure E2C). Specifically, type I (IFNβ) and type II (IFNγ) IFN-stimulated genes (e.g., *CCL18*, *IFI16*, *TLR2*, and *TLR3*) (Figure 3F) and several activation markers (e.g., *CD80*, *CD86*, and *CCL2*) were upregulated only in control animal AMs (Figure E2D). A significant number (297) of downregulated DEGs from the control animal AMs mapped to regulated exocytosis, cell morphogenesis, and response to wounding pathways (Figure E2E) such as *SIGLEC10*, *PTPN6*, and *SDC1* (Figure E2F). Next, the Chea3 (ChIP-X Enrichment Analysis 3) database (54) was used to predict the TF regulation of the DEGs. This analysis showed that genes upregulated only in control animal AMs with RSV were regulated by TFs PLSCR1, SP100, and IRF7 (which are important for phagocytosis and antiviral responses [55–58]). In contrast, genes only upregulated in EtOH AMs were regulated by TF HMGA2 associated with inflammatory responses (59) (Figure E2G). These observations suggest that chronic EtOH drinking skews AMs toward a heightened inflammatory response and away from a robust antiviral transcriptional response.

scRNA-Seq Profiling Reveals Significant Changes in AM Transcriptional Profiles with Chronic EtOH

To investigate the impact of chronic EtOH on AM cell states, we performed scRNA-Seq on $CD14^+$ purified cells from BAL samples obtained from control animals ($n = 3$ females pooled, 4 males) and EtOH animals ($n = 3$ females pooled, 2 males) (Figure E3A). Integration of replicates and further uniform manifold projection of clustering analysis revealed 11 clusters (Figure 4A; Figure E3B). Expression of major macrophage/monocyte markers identified 10 AM clusters (0, 1, 2, 3, 4, 5, 6, 8, 9, and 10; expressing high levels of *MSR1*, *MARCO*, *FABP4*, *PPARG*, *MRC1*, *LTAH4*, and *CTSD*) and 1 monocyte cluster (7; expressing high levels of *FGL2*, *MS4A6A*, *and CCL17*) (Figure E3C; Table E3). To validate our identification of cluster 7 as a monocyte cluster, we integrated single-cell profiles of BAL macrophages with those of blood monocytes from the same female animals (48) (Figure E4A). We projected cells that clustered with the blood monocytes back onto the uniform manifold projection, which revealed that cluster 7 was the major monocyte subset with some monocyte infiltration in cluster 0 (Figure E4B).

The AM clusters were further defined on the basis of their unique expression of genes and their functional implications (Figure 4B; Figure E4C). AM cluster 2 highly expressed genes associated with stress (*CD44* and *FOSB*) and cytokine responses (*PTPRC*). Clusters 3 and 4 had high expression of genes mapping to the regulation of cell adhesion

Figure 2. (*Continued*). EtOH. Scale is indicated. To the right of each is a bar chart of the reads per kilobase of transcript, per million mapped reads expression value of the gene from bulk RNA-Seq analysis. (*E*) Nonpromoter DARs were lifted over to the human genome and enriched for cis-regulatory mechanisms using GREAT (Genomic Regions Enrichment of Annotations Tool). Bubble plot of the open nonpromoter DARs with EtOH enrichment in which the size of the bubble represents the number of gene regions associated with that term and the color represents the FDR significance in which darker red indicates a more significant value. (*F*) Homer motif enrichment of all distal intergenic DARs. The percentage motif binding sites within DAR open in EtOH or control animal samples are listed.

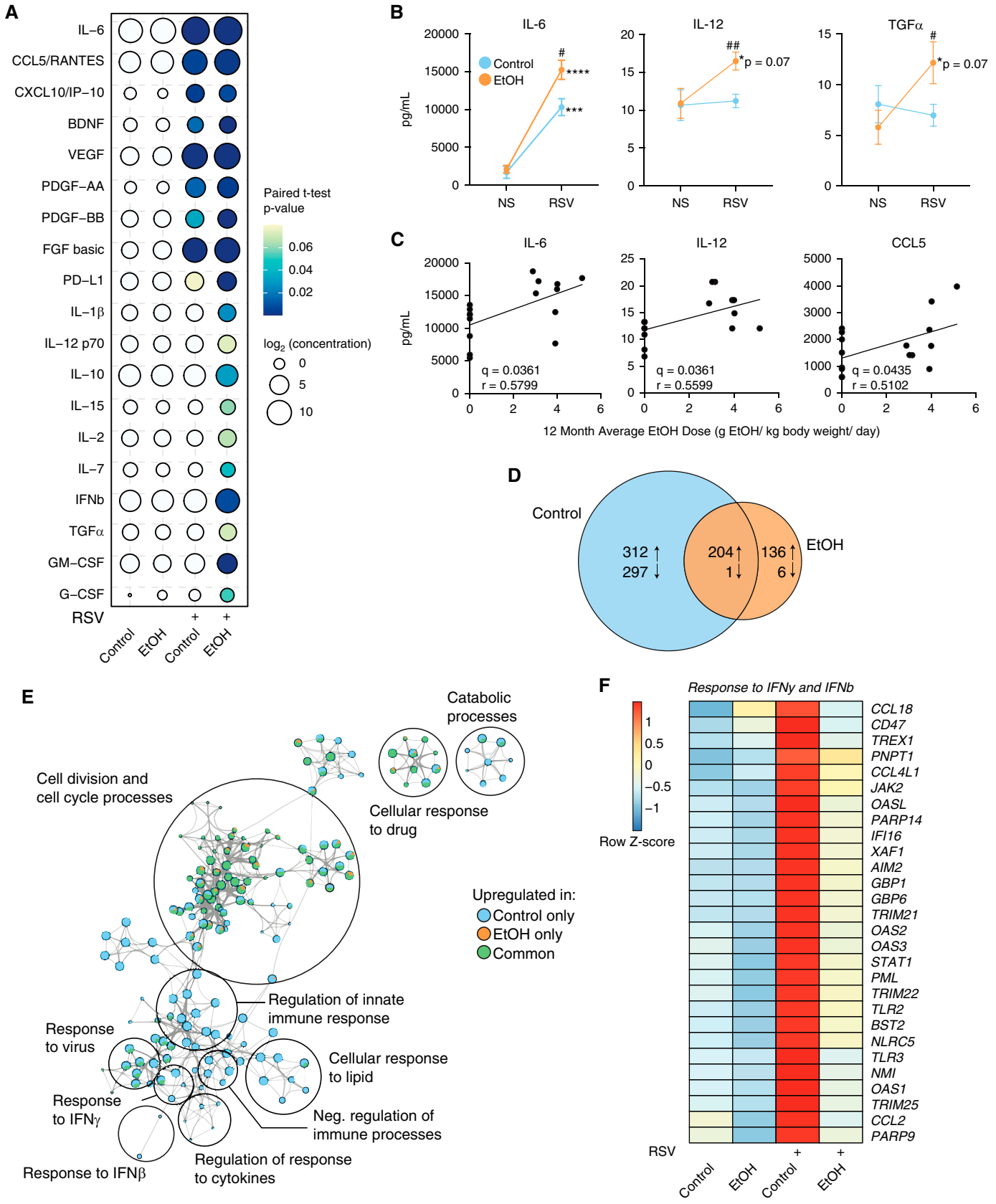

Figure 3. EtOH-induced heightened inflammatory with compromised transcriptional response to RSV. AMs were purified and stimulated with RSV for 16 hours, followed by Luminex analysis of mediator production and RNA-Seq. (*A*) Bubble plot representing immune factor production

(*S100A10* and *LGALS3*) and angiogenesis (*TGFBR3* and *GPNMB*), respectively. AM cluster 5 was characterized by high concentrations of cathepsin genes (*CTSB*, *CTSL*, and *CTSG*) associated with bacterial response processes. Cluster 9 was enriched in transcripts important for proliferation (*STMN1*, *MKI67*, and *TOP2A*) and cluster 10 with oxidative stress response (*LCN2*). AM cluster 8 was an antiviral response cluster with high expression of *ISG15*, *IFIT1*, and *IRF7*. Cluster 6 genes mapped to sterol biosynthesis (*MSMO1*, *CYP51A1*, and *SQLE*), and cluster 1 genes included *PTGDS* and *MCM7*. Finally, cluster 0 was an activated macrophage cluster expressing high concentrations of LPS responsive genes (*CLEC4E*, *S100A8*, and *S100A9*) (Figure 4B; Figure E4C).

To identify potential differentiation trajectories in the AM populations, we performed pseudotime analysis using Slingshot to set the starting point at the infiltrating monocyte cluster. This analysis revealed five unique trajectories branching from cluster 7 (Figure 4A), which all showed increased expression of tissue-resident macrophage markers (*FABP4* and *MARCO*) and decreasing monocyte markers (*CPVL* and *TMEM176B*) (Figure E4D). We profiled the cellular densities along each trajectory, which revealed a bias in cells from control animals at the start and an increase in cells from the EtOH group along the course of the pseudotime, particularly lineages 3 and 4 (Figure 4C). Lineage 3 was driven by increasing expression of oxidative stress-responsive genes (*BTG1*, *GSTP1*, *SFPG*, and *PPP1R15B*) together with tissue macrophage genes *CD163* and *MRC1* (Figure E5). Lineage 4 was driven by increased expression of *CLEC4E*, associated with inflammatory macrophage responses (Figure E5).

We finally examined the redistribution of AM populations with EtOH (Figure 4D). A modest increase in AM cluster 0 was accompanied by a significant decrease in AM cluster 3 with chronic EtOH drinking (Figure 4D). Functional enrichment showed that defining genes for cluster 0 were associated with apoptosis and responses to bacterial and fungal pathogens, whereas cluster 3 defining genes were associated with membrane raft organization, regulation of fibroblast proliferation, and cell adhesion (Figure 4E). In addition, as we found increased accessibility of the cathepsin G promoter and corresponding baseline RNA expression, we profiled the expression of *CTSG* from the scRNA-Seq data and found that AM clusters 1 and 5 had significantly elevated expression of *CTSG* with EtOH (Figure E6A). Together with the bulk RNA-Seq data, these observations suggest that chronic EtOH induces transcriptional shifts in AM cell states indicative of a reduced tissue repair capacity and antimicrobial response and heightened inflammatory state.

EtOH-induced Oxidative Stress Alters AM Metabolic-associated Processes and Functional Abilities

To determine the potential functional implications of EtOH-induced changes in AMs, we first assessed differential gene expression across aggregated single-cell clusters (Figure 5A). Functional enrichment of the DEGs downregulated with EtOH mapped to GO terms "monocyte chemotaxis" (e.g., *LGMN* and *CCL2*), "angiogenesis" (e.g., *ANPEP* and *ECM1*), and "epithelial cell proliferation" (e.g., *GRN* and *CCL24*) (Figure 5A). On the other hand, upregulated DEGs enriched to "oxidative phosphorylation" (e.g., *COX7A1*, *ATP8*, and *ND4*), "regulation of apoptosis" (e.g., *CD74*, *RPL11*, and *PPIA*), and "antigen processing and presentation" (e.g., *B2M* and *FCER1G*) (Figure 5A). In line with the significant upregulation of genes that enriched to GO term "oxidative phosphorylation," the module scores for "oxidative stress" and "HIF1A signaling" were also elevated with EtOH (Figure 5B; Figure E6B; Table E4). Oxidative phosphorylation is a critical energy (ATP)-generating metabolic pathway that occurs within the mitochondria (60). Therefore, we assessed the impact of chronic EtOH drinking on mitochondrial activity using flow cytometry. Mitochondrial membrane potential was significantly increased with EtOH in AMs but remained comparable in the interstitial macrophage subset (Figure 5C; Figure E6C). Moreover, concentrations of intracellular ROS in AMs and interstitial macrophages were significantly increased after stimulation with LPS (Figure 5D; Figure E6D). As EtOH-induced oxidative stress has been shown to affect the phagocytic capacity of AMs (61, 62), we compared the module score for phagocytosis determined from scRNA-Seq data between the two groups. Both the module score as well as the ability of AMs to phagocytose pHrodo-labeled *S. aureus* were significantly reduced with EtOH drinking (Figures 5E and 5F). Finally, in line with the exaggerated inflammatory response to LPS and RSV stimulation, the cytokine signaling module score was increased in AM with EtOH (Figure E6E). In summary, EtOH drinking induces oxidative stress in AMs, leading to increased ROS production and mitochondrial activity coupled with reduced phagocytosis capacity and increased inflammatory gene expression.

Discussion

Tissue-resident macrophages and infiltrating monocytes make up a majority of the immune cells in the alveolar space, where they respond to insults to the respiratory tract, including toxins, pathogens, and

Figure 3. (*Continued*). (pg/ml) in the presence or absence of RSV by AMs from control animals and EtOH animals. The size of each circle represents the $\log_2$ average concentration of the indicated secreted factor, and the color denotes the *P* value significance, in which darker blue represents a more significant value. The *P* values were calculated between the unstimulated and stimulated conditions for each group using paired *t* test. White circles indicate an uncalculated or nonsignificant *P* value. (*B*) Line plots represent the Luminex data for the selected analytes. Significance was tested by paired *t* test (*) or unpaired *t* test (#) with Welch's correction. (*C*) Scatter plots showing correlation analysis of selected factor concentration with a dose of EtOH (g EtOH/kg body weight/day). Corrected *P* value (*q*, Benjamini and Hochberg) and Pearson *r* value are indicated. (*D*) Venn diagram comparing up and downregulated DEGs after RSV stimulation in control animal and EtOH animal AMs. (*E*) Cytoscape plot of functional enrichment to GO biological processes of upregulated DEGs with RSV from both groups compared with unstimulated conditions. The size of the dot represents the number of genes enriching to that term, and the pie chart filling represents the contribution of DEGs from each group. Related processes are grouped into the larger terms circled. (*F*) Heatmap representing the averaged expression of DEGs in each group/stimulation condition from the *Response to IFNγ* and *Response to IFNb* GO terms in which the scale is row *Z*-score representing low (blue) and high (red) expression. $^{\#}P < 0.05$, $^{\#\#}P < 0.01$, $^{***}P < 0.001$, and $^{****}P < 0.0001$. BDNF = brain-derived neurotrophic factor; FGF = fibroblast growth factor; G-CSF = granulocyte colony-stimulating factor; GM-CSF = granulocyte-macrophage colony-stimulating factor; NS = no stimulation; PDGF = platelet-derived growth factor; VEGF = vascular endothelial growth factor.

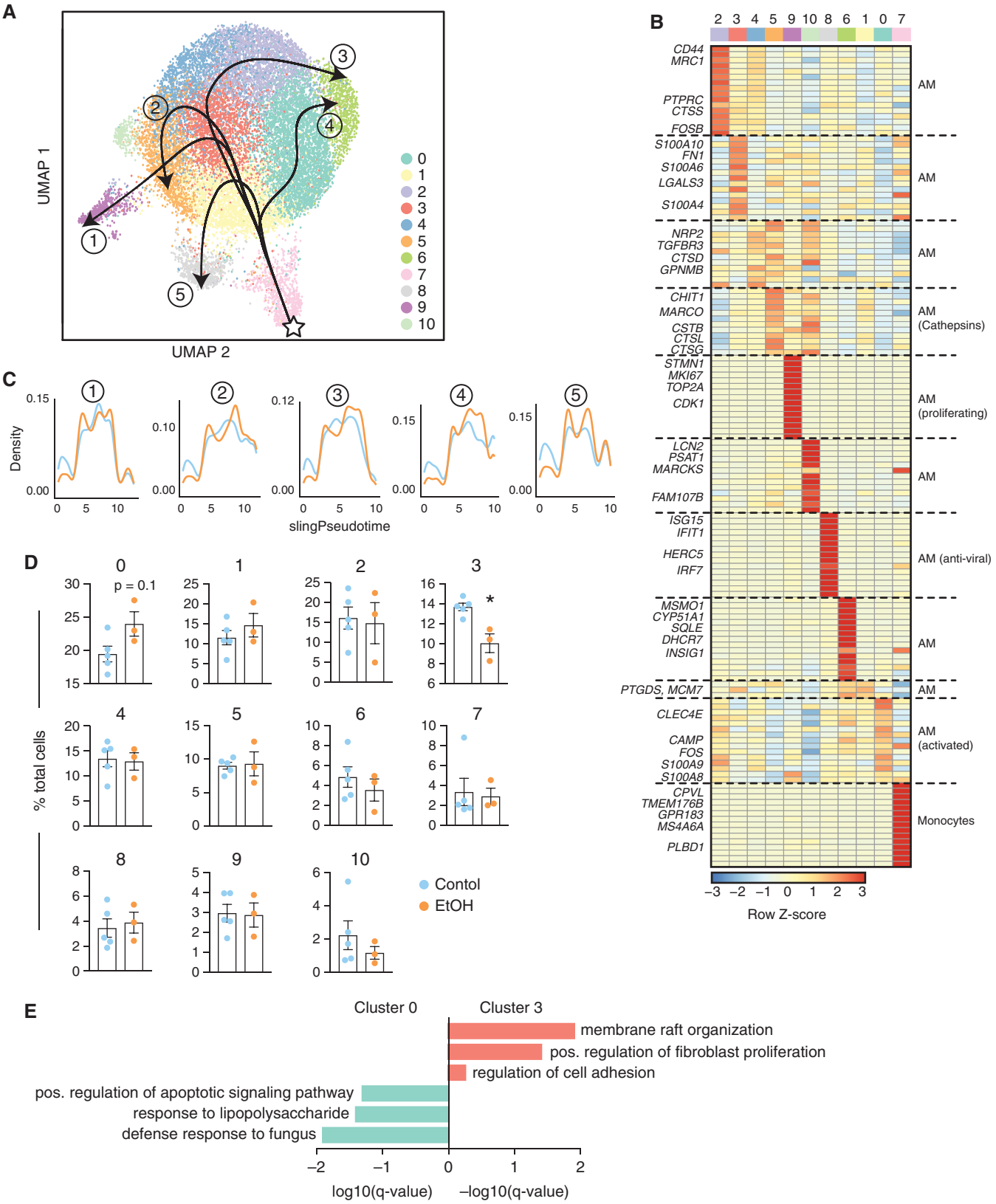

Figure 4. scRNA-Seq profiling of AMs after chronic EtOH drinking. Macrophages and monocytes ($n = 3$ control female pooled, 4 control male/3 EtOH female pooled, 2 EtOH male) were purified from total BAL and subjected to 10X scRNA-Seq analysis. (*A*) Visualization of total cells by

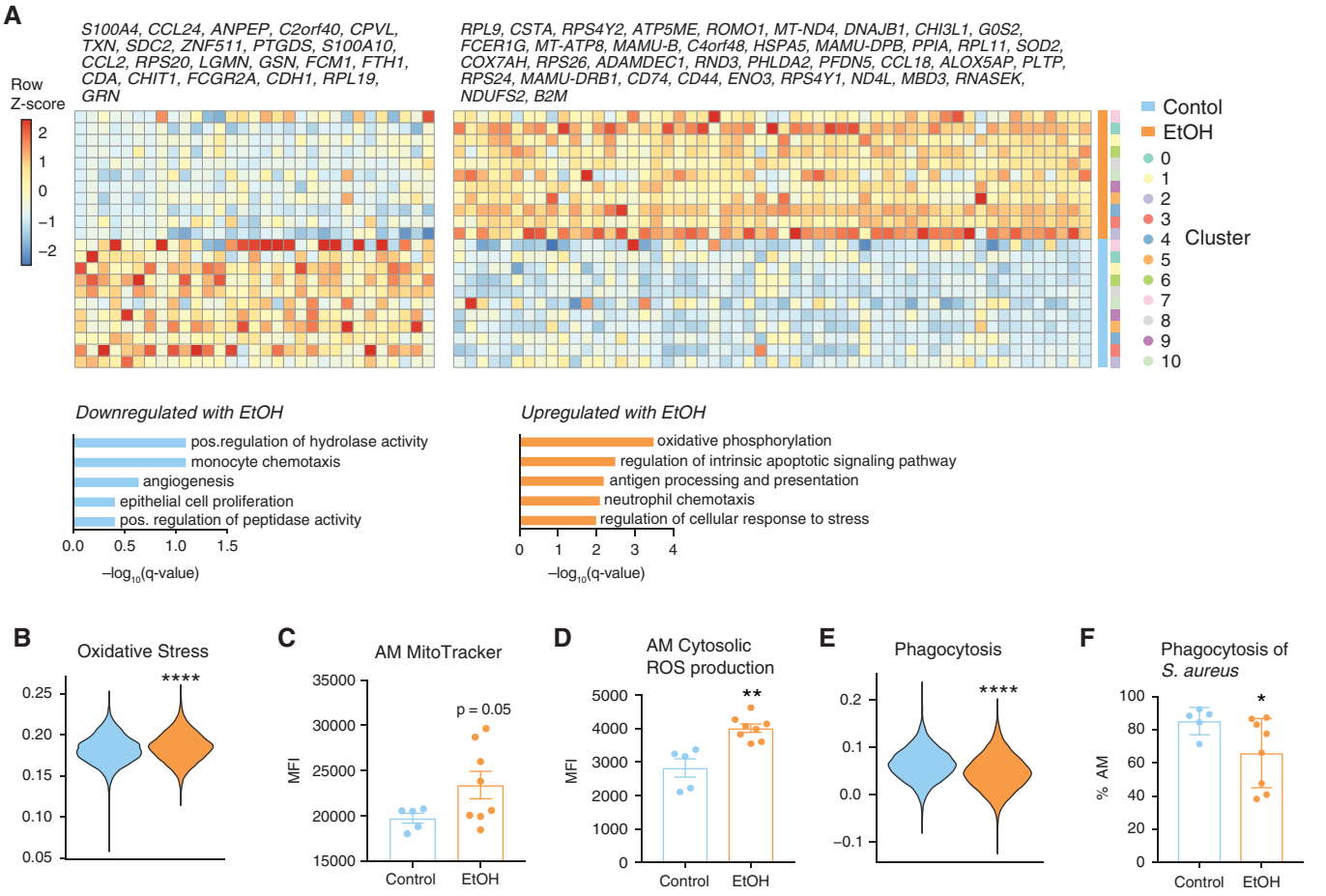

Figure 5. Chronic EtOH drinking leads to increased oxidative stress accompanied by functional defects in AMs. (*A*) Heatmap (top) representing the averaged expression of DEGs between control animal and EtOH animal AMs identified using the *FindMarkers* function in which the scale is row *Z*-score representing low (blue) and high (red) expression. Bar plots (bottom) showing GO biological processes enriched in down (left)- or up (right)-regulated genes. (*B*) Violin plot representing oxidative stress module scoring of total cells from each group. Significance was calculated using the Mann-Whitney test. (*C*) Bar plot showing MFIs of intracellular mitochondrial membrane potential stained with MitoTracker Red in AMs. (*D*) Bar plot showing MFI of intracellular ROS stained by CellROX Deep Red Reagent in AMs. (*E*) Violin plot representing phagocytosis module scoring of total cells from each group. Significance was calculated using the Mann-Whitney test. (*F*) Bar plot representing the percentage of AMs positive for pHrodo Red *Staphylococcus aureus* particles. Unless indicated, statistical significance was calculated using *t* test with Welch's correction. $^{*}P < 0.05$, $^{**}P < 0.01$, and $^{****}P < 0.0001$.

allergens (63). They are responsible for both inflammatory responses as well as tissue remodeling and repair. Under homeostatic conditions, a tight balance between inflammatory and antiinflammatory responses is maintained. This delicate balance can be dysregulated by environmental factors, including pollutants, smoking, and alcohol drinking (64). In fact, chronic heavy alcohol drinking results in increased susceptibility to respiratory diseases (10–16), but the mechanisms underlying this increased vulnerability are not completely understood.

In this study, we performed a comprehensive examination of the impact of chronic heavy alcohol drinking on the transcriptome, epigenome, and function of AMs obtained from a rhesus model of voluntary ethanol self-administration. This model accurately recapitulates human drinking behavior in duration and dose and represents a chronic, not acute, model of the effects of alcohol and its metabolites on the

Figure 4. (*Continued*). UMAP colored by cluster overlayed with indicated pseudotime lineages identified by Slingshot trajectory analysis. (*B*) Heatmap represents the averaged expression of cluster marker genes identified using the *FindMarkers* function in which the scale is row *Z*-score representing low (blue) and high (red) expression. (*C*) Cell density plots for control and EtOH groups across each of five trajectory lineages determined by Slingshot. (*D*) Bar graphs showing the relative abundance of the cells from control (blue) or EtOH (orange) groups within each identified cluster. Significance was calculated by *t* test with Welch's correction. (*E*) Bar plots showing GO functional enrichment terms for clusters 0 and 3 genes identified using the *FindAllMarkers* function in which the *x*-axis is the $\log_{10}$ or $-\log_{10}$ (*q*-value). UMAP = uniform manifold approximation and projection.

body. Consequently, this study design allows us to interrogate the pleiotropic impact of chronic voluntary ethanol consumption on various organ systems in a genetically outbred animal model while avoiding several confounders that are difficult to control in clinical studies. Although the genetic diversity of the animal species and voluntary ethanol consumption are major strengths of this model, they can also lead to increased intragroup variability. To understand how chronic ethanol consumption impacted lung immunity, BALs were obtained from male and female rhesus macaques after 12 months of heavy drinking (>3 g EtOH per kg body weight per day or >12 drinks per day for an average 60 kg human). Our findings suggest that chronic EtOH drinking alters the epigenetic and transcriptional landscapes of AMs, skewing them away from tissue maintenance/repair and antimicrobial defenses and toward heightened inflammatory responses. In support of these genomic findings, functional assays show increased inflammatory mediator responses to microbial stimulations, dysregulated transcriptional responses to viruses, and reduced phagocytic capacity in AMs with EtOH drinking.

It has been previously reported that AMs from patients with alcohol use disorders express elevated levels of inflammatory mediators (65, 66) as well as reduced phagocytic ability in AMs with chronic drinking (26, 64). Similarly, here we show that AMs from EtOH-drinking animals generated a hyperinflammatory cytokine and chemokine response to LPS. These observations are in line with data from our earlier studies that reported exaggerated inflammatory responses by splenic macrophage and blood monocyte responses to LPS (46, 48, 67), as well as studies on long-term EtOH exposure and increased inflammatory responses in myeloid cells (53). To determine if this hyperresponsiveness extended to a relevant lung pathogen, we stimulated AMs with RSV. AMs from EtOH animals produced significantly higher concentrations of IL-6, IL-12, and TGFα than control animals. Increased production of IL-6 in response to RSV with EtOH could indicate broad hyperinflammation. However, as IL-12 and TGFα concentrations are not increased in control AMs after RSV stimulation, we believe the production of increased concentrations of these factors with EtOH to be indicative of a dysregulated response. In line with the aberrant inflammatory responses, the scRNA-Seq analysis showed an increase in the abundance of an AM cluster expressing high levels of inflammatory genes and increased scores of cytokine signaling modules. In addition, TF motif analysis revealed enrichment of binding sites for TF AP-1, IRF8, and NFκB with chronic EtOH drinking. Similarly, we previously reported changes in splenic macrophages and circulating monocytes from alcohol-consuming macaques, thus indicating broad epigenetic rewiring by chronic drinking (46, 67).

The transcriptional profiles of the AMs after RSV infection showed a reduced induction of interferon-stimulated genes, indicating disruptions in antiviral immunity. Indeed, individuals with alcohol use disorders have shown increased susceptibility to RSV (10, 11). Coinciding with this finding, promoter regions that mapped to T-helper cell differentiation and regulation of cell migration were repressed in AMs from EtOH-drinking animals, indicating suppression of secondary immune activation processes. In addition, phagocytosis module score and ability to uptake pHrodo labeled *S. aureus* were compromised in AMs from EtOH-consuming animals as previously observed in cell culture and rodent models (64, 68). Collectively, these alterations at baseline suggest that AMs are poised toward a heightened inflammatory state and away from antimicrobial responses.

One suggested mechanism of reduced phagocytosis in AMs with EtOH is oxidative stress induced by increased nicotinamide adenine dinucleotide phosphate oxidase (61, 62, 69). scRNA-Seq data showed increased oxidative stress module scores in AMs from EtOH animals. Prior studies have reported a link between EtOH and its metabolites and ROS production (70) and oxidative stress (71). As ROSs serve as inflammasome-activating signals and induce inflammation (72), this could contribute to the exaggerated production of cytokines and chemokines in response to stimulation. Because oxidative phosphorylation is linked to mitochondrial activation, we assessed changes in mitochondrial content, which was indeed increased with chronic EtOH consumption. Future studies would be needed to determine the bioenergetics of these mitochondria and how they are contributing to increased ROS levels and further inflammation in AMs (73).

Another critical function of AMs is the resolution of inflammation and tissue repair in which patients with alcohol use disorders have a higher risk of developing acute respiratory distress syndrome (10, 18) and compromised wound healing responses (74). Bulk RNA-Seq of AMs revealed decreased expression of genes mapping to wound healing and epithelial cell proliferation processes in EtOH AMs. Similarly, scRNA-Seq data also suggest reduced fibroblast and epithelial cell maintenance potential. These changes may be mediated epigenetically because reduced chromatin accessibility was noted in promoters that regulate genes important for endothelium development and cell junction assembly with EtOH.

scRNA-Seq data revealed significant heterogeneity within tissue-resident and monocyte-derived macrophage populations. Recent studies on human lung macrophages have also shown significant macrophage diversity with disease states (30). Clusters that were abundant with EtOH drinking exhibited a transcriptional profile consistent with a heightened inflammatory state. Trajectory analysis suggests the potential accumulation of highly differentiated macrophages with chronic EtOH. Although activation and differentiation of macrophages are controlled by complex epigenetic mechanisms (75), it is possible that the exacerbated inflammatory responses observed with EtOH can be attributed to a process akin to "innate training" in which environmental factors lead to epigenetic changes that have long-lasting functional consequences (76). However, more targeted studies would be needed to confirm this hypothesis, including an analysis of specific histone modifications.

An intriguing observation throughout this study is the increased expression of cathepsin G (*CTSG*) in AMs detected by bulk RNA-Seq and scRNA-Seq accompanied by increased chromatin accessibility at *CTSG* promoter with chronic EtOH drinking. Cathepsins are proteases active in low pH lysosomes and have versatile functions in innate immunity, activation, and tissue degradation (77). Dysregulated expression of cathepsins has been linked to diseases including arthritis, muscular dystrophy, and tuberculosis (77). The significance of alcohol-induced increased cathepsin expression in AMs needs to be further studied to determine its importance in AM function and lung immunity.

Conclusions

This study provides a comprehensive examination of AMs in the context of chronic alcohol drinking in macaques. We acknowledge several limitations, including the use of LPS instead of a bacterial pathogen and biological variability within samples owing to the outbred macaque model. Potential new targets identified here include increased mitochondrial activation, increased ROS production, and epigenetic alterations. These altered AM states could contribute to the increased susceptibility of patients with alcohol use disorders to respiratory infections. ■

Author disclosures are available with the text of this article at www.atsjournals.org.

Acknowledgment: The authors thank the members of the Grant laboratory for expert animal care and sample procurement. The authors thank Dr. Jennifer Atwood for assistance with sorting in the flow cytometry core at the Institute for Immunology, University of California, Irvine (UCI). The authors thank Dr. Melanie Oakes from UCI Genomics and High-Throughput Facility for assistance with 10X library preparation and sequencing.

References

1. O'Keefe JH, Bhatti SK, Bajwa A, DiNicolantonio JJ, Lavie CJ. Alcohol and cardiovascular health: the dose makes the poison … or the remedy. *Mayo Clin Proc* 2014;89:382–393.
2. Mukamal KJ, Rimm EB. Alcohol's effects on the risk for coronary heart disease. *Alcohol Res Health* 2001;25:255–261.
3. Fedirko V, Tramacere I, Bagnardi V, Rota M, Scotti L, Islami F, *et al.* Alcohol drinking and colorectal cancer risk: an overall and dose–response meta-analysis of published studies. *Ann Oncol* 2011;22: 1958–1972.
4. Baan R, Straif K, Grosse Y, Secretan B, El Ghissassi F, Bouvard V, *et al.*; WHO International Agency for Research on Cancer Monograph Working Group. Carcinogenicity of alcoholic beverages. *Lancet Oncol* 2007;8: 292–293.
5. Grewal P, Viswanathen VA. Liver cancer and alcohol. *Clin Liver Dis* 2012; 16:839–850.
6. Priddy BM, Carmack SA, Thomas LC, Vendruscolo JC, Koob GF, Vendruscolo LF. Sex, strain, and estrous cycle influences on alcohol drinking in rats. *Pharmacol Biochem Behav* 2017;152:61–67.
7. Bruha R, Dvorak K, Petrtyl J. Alcoholic liver disease. *World J Hepatol* 2012;4:81–90.
8. O'Brien JM Jr, Lu B, Ali NA, Levine DA, Aberegg SK, Lemeshow S. Insurance type and sepsis-associated hospitalizations and sepsis-associated mortality among U.S. adults: a retrospective cohort study. *Crit Care* 2011;15:R130.
9. Mokdad AH, Marks JS, Stroup DF, Gerberding JL. Actual causes of death in the United States, 2000. *JAMA* 2004;291:1238–1245.
10. Simet SM, Sisson JH. Alcohol's effects on lung health and immunity. *Alcohol Res* 2015;37:199–208.
11. Jerrells TR, Pavlik JA, DeVasure J, Vidlak D, Costello A, Strachota JM, *et al.* Association of chronic alcohol consumption and increased susceptibility to and pathogenic effects of pulmonary infection with respiratory syncytial virus in mice. *Alcohol* 2007;41:357–369.
12. Saitz R, Ghali WA, Moskowitz MA. The impact of alcohol-related diagnoses on pneumonia outcomes. *Arch Intern Med* 1997;157: 1446–1452.
13. Samokhvalov AV, Irving HM, Rehm J. Alcohol consumption as a risk factor for pneumonia: a systematic review and meta-analysis. *Epidemiol Infect* 2010;138:1789–1795.
14. Luján M, Gallego M, Belmonte Y, Fontanals D, Vallès J, Lisboa T, *et al.* Influence of pneumococcal serotype group on outcome in adults with bacteremic pneumonia. *Eur Respir J* 2010;36:1073–1079.
15. Buskin SE, Gale JL, Weiss NS, Nolan CM. Tuberculosis risk factors in adults in King County, Washington, 1988 through 1990. *Am J Public Health* 1994;84:1750–1756.
16. Narasimhan P, Wood J, Macintyre CR, Mathai D. Risk factors for tuberculosis. *Pulm Med* 2013;2013:828939.
17. Moss M, Bucher B, Moore FA, Moore EE, Parsons PE. The role of chronic alcohol abuse in the development of acute respiratory distress syndrome in adults. *JAMA* 1996;275:50–54.
18. Moss M, Burnham EL. Chronic alcohol abuse, acute respiratory distress syndrome, and multiple organ dysfunction. *Crit Care Med* 2003;31 (4, Suppl):S207–S212.
19. Simou E, Leonardi-Bee J, Britton J. The effect of alcohol consumption on the risk of ARDS: a systematic review and meta-analysis. *Chest* 2018;154:58–68.
20. Sisson JH. Ethanol stimulates apparent nitric oxide-dependent ciliary beat frequency in bovine airway epithelial cells. *Am J Physiol* 1995;268: L596–L600.
21. Sisson JH, Pavlik JA, Wyatt TA. Alcohol stimulates ciliary motility of isolated airway axonemes through a nitric oxide, cyclase, and cyclic nucleotide-dependent kinase mechanism. *Alcohol Clin Exp Res* 2009; 33:610–616.
22. Wyatt TA, Sisson JH. Chronic ethanol downregulates PKA activation and ciliary beating in bovine bronchial epithelial cells. *Am J Physiol Lung Cell Mol Physiol* 2001;281:L575–L581.
23. Guidot DM, Modelska K, Lois M, Jain L, Moss IM, Pittet JF, *et al.* Ethanol ingestion via glutathione depletion impairs alveolar epithelial barrier function in rats. *Am J Physiol Lung Cell Mol Physiol* 2000;279: L127–L135.
24. Simet SM, Wyatt TA, DeVasure J, Yanov D, Allen-Gipson D, Sisson JH. Alcohol increases the permeability of airway epithelial tight junctions in Beas-2B and NHBE cells. *Alcohol Clin Exp Res* 2012;36:432–442.
25. Rubins JB. Alveolar macrophages: wielding the double-edged sword of inflammation. *Am J Respir Crit Care Med* 2003;167:103–104.
26. D'Souza NB, Nelson S, Summer WR, Deaciuc IV. Alcohol modulates alveolar macrophage tumor necrosis factor-alpha, superoxide anion, and nitric oxide secretion in the rat. *Alcohol Clin Exp Res* 1996;20: 156–163.
27. Craig A, Mai J, Cai S, Jeyaseelan S. Neutrophil recruitment to the lungs during bacterial pneumonia. *Infect Immun* 2009;77:568–575.
28. Joshi PC, Applewhite L, Ritzenthaler JD, Roman J, Fernandez AL, Eaton DC, *et al.* Chronic ethanol ingestion in rats decreases granulocyte-macrophage colony-stimulating factor receptor expression and downstream signaling in the alveolar macrophage. *J Immunol* 2005; 175:6837–6845.
29. Liang Y, Harris FL, Brown LA. Alcohol-induced mitochondrial oxidative stress and alveolar macrophage dysfunction. *BioMed Res Int* 2014; 2014:371593.
30. Evren E, Ringqvist E, Willinger T. Origin and ontogeny of lung macrophages: from mice to humans. *Immunology* 2020;160:126–138.
31. Kopf M, Schneider C, Nobs SP. The development and function of lung-resident macrophages and dendritic cells. *Nat Immunol* 2015;16:36–44.
32. Joshi N, Walter JM, Misharin AV. Alveolar macrophages. *Cell Immunol* 2018;330:86–90.
33. Hussell T, Bell TJ. Alveolar macrophages: plasticity in a tissue-specific context. *Nat Rev Immunol* 2014;14:81–93.
34. Hetzel M, Ackermann M, Lachmann N. Beyond "big eaters": the versatile role of alveolar macrophages in health and disease. *Int J Mol Sci* 2021; 22:3308.
35. Garbi N, Lambrecht BN. Location, function, and ontogeny of pulmonary macrophages during the steady-state. *Pflugers Arch* 2017;469: 561–572.
36. Varol C, Mildner A, Jung S. Macrophages: development and tissue specialization. *Annu Rev Immunol* 2015;33:643–675.
37. Tan SY, Krasnow MA. Developmental origin of lung macrophage diversity. *Development* 2016;143:1318–1327.

38. Robinson MD, McCarthy DJ, Smyth GK. edgeR: a Bioconductor package for differential expression analysis of digital gene expression data. *Bioinformatics* 2010;26:139–140.
39. Zhou Y, Zhou B, Pache L, Chang M, Khodabakhshi AH, Tanaseichuk O, *et al.* Metascape provides a biologist-oriented resource for the analysis of systems-level datasets. *Nat Commun* 2019;10:1523.
40. Heinz S, Benner C, Spann N, Bertolino E, Lin YC, Laslo P, *et al.* Simple combinations of lineage-determining transcription factors prime cis-regulatory elements required for macrophage and B cell identities. *Mol Cell* 2010;38:576–589.
41. Stuart T, Butler A, Hoffman P, Hafemeister C, Papalexi E, Mauck, *et al.* Comprehensive integration of single-cell data. *Cell* 2019;177: 1888–1902, e21.
42. Street K, Risso D, Fletcher RB, Das D, Ngai J, Yosef N, *et al.* Slingshot: cell lineage and pseudotime inference for single-cell transcriptomics. *BMC Genomics* 2018;19:477.
43. Bharat A, Bhorade SM, Morales-Nebreda L, McQuattie-Pimentel AC, Soberanes S, Ridge K, *et al.* Flow cytometry reveals similarities between lung macrophages in humans and mice. *Am J Respir Cell Mol Biol* 2016;54:147–149.
44. Cai Y, Sugimoto C, Arainga M, Alvarez X, Didier ES, Kuroda MJ. In vivo characterization of alveolar and interstitial lung macrophages in rhesus macaques: implications for understanding lung disease in humans. *J Immunol* 2014;192:2821–2829.
45. Hunegnaw R, Mushtaq Z, Enyindah-Asonye G, Hoang T, Robert-Guroff M. Alveolar macrophage dysfunction and increased PD-1 expression during chronic SIV infection of rhesus macaques. *Front Immunol* 2019; 10:1537.
46. Sureshchandra S, Stull C, Ligh BJK, Nguyen SB, Grant KA, Messaoudi I. Chronic heavy drinking drives distinct transcriptional and epigenetic changes in splenic macrophages. *EBioMedicine* 2019;43:594–606.
47. Sureshchandra S, Rais M, Stull C, Grant K, Messaoudi I. Transcriptome profiling reveals disruption of innate immunity in chronic heavy ethanol consuming female rhesus macaques. *PLoS One* 2016;11: e0159295.
48. Lewis SA, Sureshchandra S, Doratt B, Jimenez VA, Stull C, Grant KA, *et al.* Transcriptional, epigenetic, and functional reprogramming of monocytes from non-human primates following chronic alcohol drinking. *Front Immunol* 2021;12:724015.
49. Baek YS, Haas S, Hackstein H, Bein G, Hernandez-Santana M, Lehrach H, *et al.* Identification of novel transcriptional regulators involved in macrophage differentiation and activation in U937 cells. *BMC Immunol* 2009;10:18.
50. Rosa BA, Ahmed M, Singh DK, Choreño-Parra JA, Cole J, Jiménez-Álvarez LA, *et al.* IFN signaling and neutrophil degranulation transcriptional signatures are induced during SARS-CoV-2 infection. *Commun Biol* 2021;4:290.
51. Makita N, Hizukuri Y, Yamashiro K, Murakawa M, Hayashi Y. IL-10 enhances the phenotype of M2 macrophages induced by IL-4 and confers the ability to increase eosinophil migration. *Int Immunol* 2015; 27:131–141.
52. Sureshchandra S, Raus A, Jankeel A, Ligh BJK, Walter NAR, Newman N, *et al.* Dose-dependent effects of chronic alcohol drinking on peripheral immune responses. *Sci Rep* 2019;9:7847.
53. Szabo G, Saha B. Alcohol's effect on host defense. *Alcohol Res* 2015;37: 159–170.
54. Keenan AB, Torre D, Lachmann A, Leong AK, Wojciechowicz ML, Utti V, *et al.* ChEA3: transcription factor enrichment analysis by orthogonal omics integration. *Nucleic Acids Res* 2019;47:W212–W224.
55. Herate C, Ramdani G, Grant NJ, Marion S, Gasman S, Niedergang F, *et al.* Phospholipid scramblase 1 modulates FcR-mediated phagocytosis in differentiated macrophages. *PLoS One* 2016;11: e0145617.
56. Lu R, Pitha PM. Monocyte differentiation to macrophage requires interferon regulatory factor 7. *J Biol Chem* 2001;276:45491–45496.
57. Sin WX, Yeong JP, Lim TJF, Su IH, Connolly JE, Chin KC. IRF-7 mediates type I IFN responses in endotoxin-challenged mice. *Front Immunol* 2020;11:640.
58. Xia C, Braunstein Z, Toomey AC, Zhong J, Rao X. S100 proteins as an important regulator of macrophage inflammation. *Front Immunol* 2018; 8:1908.
59. Huang H, Li H, Chen X, Yang Y, Li X, Li W, *et al.* HMGA2, a driver of inflammation, is associated with hypermethylation in acute liver injury. *Toxicol Appl Pharmacol* 2017;328:34–45.
60. Angajala A, Lim S, Phillips JB, Kim JH, Yates C, You Z, *et al.* Diverse roles of mitochondria in immune responses: novel insights into immuno-metabolism. *Front Immunol* 2018;9:1605.
61. Yeligar SM, Harris FL, Hart CM, Brown LA. Glutathione attenuates ethanol-induced alveolar macrophage oxidative stress and dysfunction by downregulating NADPH oxidases. *Am J Physiol Lung Cell Mol Physiol* 2014;306:L429–L441.
62. Yeligar SM, Harris FL, Hart CM, Brown LA. Ethanol induces oxidative stress in alveolar macrophages via upregulation of NADPH oxidases. *J Immunol* 2012;188:3648–3657.
63. Baharom F, Rankin G, Blomberg A, Smed-Sörensen A. Human lung mononuclear phagocytes in health and disease. *Front Immunol* 2017;8:499.
64. Karavitis J, Kovacs EJ. Macrophage phagocytosis: effects of environmental pollutants, alcohol, cigarette smoke, and other external factors. *J Leukoc Biol* 2011;90:1065–1078.
65. Burnham EL, Kovacs EJ, Davis CS. Pulmonary cytokine composition differs in the setting of alcohol use disorders and cigarette smoking. *Am J Physiol Lung Cell Mol Physiol* 2013;304:L873–L882.
66. O'Halloran EB, Curtis BJ, Afshar M, Chen MM, Kovacs EJ, Burnham EL. Alveolar macrophage inflammatory mediator expression is elevated in the setting of alcohol use disorders. *Alcohol* 2016;50:43–50.
67. Lewis SA, Sureshchandra S, Doratt B, Jimenez VA, Stull C, Grant KA, *et al.* Transcriptional, epigenetic, and functional reprogramming of blood monocytes in non-human primates following chronic alcohol drinking. *bioRxiv* 2021;12:724015.
68. Karavitis J, Murdoch EL, Deburghgraeve C, Ramirez L, Kovacs EJ. Ethanol suppresses phagosomal adhesion maturation, Rac activation, and subsequent actin polymerization during FcγR-mediated phagocytosis. *Cell Immunol* 2012;274:61–71.
69. Yeligar SM, Mehta AJ, Harris FL, Brown LA, Hart CM. Peroxisome proliferator-activated receptor γ regulates chronic alcohol-induced alveolar macrophage dysfunction. *Am J Respir Cell Mol Biol* 2016;55: 35–46.
70. Zakhari S. Alcohol metabolism and epigenetics changes. *Alcohol Res* 2013;35:6–16.
71. Das SK, Vasudevan DM. Alcohol-induced oxidative stress. *Life Sci* 2007; 81:177–187.
72. Harijith A, Ebenezer DL, Natarajan V. Reactive oxygen species at the crossroads of inflammasome and inflammation. *Front Physiol* 2014;5:352.
73. Morris NL, Harris FL, Brown LAS, Yeligar SM. Alcohol induces mitochondrial derangements in alveolar macrophages by upregulating NADPH oxidase 4. *Alcohol* 2021;90:27–38.
74. Jung MK, Callaci JJ, Lauing KL, Otis JS, Radek KA, Jones MK, *et al.* Alcohol exposure and mechanisms of tissue injury and repair. *Alcohol Clin Exp Res* 2011;35:392–399.
75. Chen S, Yang J, Wei Y, Wei X. Epigenetic regulation of macrophages: from homeostasis maintenance to host defense. *Cell Mol Immunol* 2020;17:36–49.
76. Saeed S, Quintin J, Kerstens HH, Rao NA, Aghajanirefah A, Matarese F, *et al.* Epigenetic programming of monocyte-to-macrophage differentiation and trained innate immunity. *Science* 2014;345:1251086.
77. Patel S, Homaei A, El-Seedi HR, Akhtar N. Cathepsins: proteases that are vital for survival but can also be fatal. *Biomed Pharmacother* 2018; 105:526–532.